

## RESEARCH ARTICLE

# AI-Based Investigation and Mitigation of Rain Effect on Channel Performance With Aid of a Novel 3D Slot Array Antenna Design for High Throughput Satellite System

ALI M. AL-SAEGH<sup>1</sup>, FATMA TAHER<sup>2</sup>, (Senior Member, IEEE), TAHA A. ELWI<sup>3</sup>,  
MOHAMMAD ALIBAKHSHIKENARI<sup>4</sup>, (Member, IEEE),  
BAL S. VIRDEE<sup>5</sup>, (Senior Member, IEEE), OSAMA ABDULLAH<sup>6</sup>, SALAHUDDIN KHAN<sup>7</sup>,  
PATRIZIA LIVRERI<sup>8</sup>, (Senior Member, IEEE),  
ABDULMAJEED AL-JUMAILY<sup>4</sup>, (Senior Member, IEEE), MOHAMED FATHY ABO SREE<sup>9</sup>,  
ARKAN MOUSA MAJEED<sup>10</sup>, LIDA KOUHALVANDI<sup>11</sup>, (Senior Member, IEEE),  
ZAID A. ABDUL HASSAIN<sup>10</sup>, AND GIOVANNI PAU<sup>12</sup>, (Senior Member, IEEE)

<sup>1</sup>Department of Space Technology Engineering, Electrical Engineering Technical College, Middle Technical University, Baghdad 10001, Iraq

<sup>2</sup>College of Technological Innovation, Zayed University, Dubai, United Arab Emirates

<sup>3</sup>International Applied and Theoretical Research Center (IATRC), Baghdad Quarter, Baghdad 10001, Iraq

<sup>4</sup>Department of Signal Theory and Communications, Universidad Carlos III de Madrid, Leganés, 28911 Madrid, Spain

<sup>5</sup>Center for Communications Technology, London Metropolitan University, N7 8DB London, U.K.

<sup>6</sup>Ministry of Higher Education and Scientific Research, Baghdad 10071, Iraq

<sup>7</sup>College of Engineering, King Saud University, Riyadh 11421, Saudi Arabia

<sup>8</sup>Department of Engineering, University of Palermo, Palermo, 90128 Sicily, Italy

<sup>9</sup>Department of Electronics and Communications Engineering, Arab Academy for Science, Technology and Maritime Transport, Cairo 11865, Egypt

<sup>10</sup>Department of Electrical Engineering, Mustansiriyah University, Baghdad 14022, Iraq

<sup>11</sup>Department of Electrical and Electronics Engineering, Dogus University, 34775 Istanbul, Turkey

<sup>12</sup>Faculty of Engineering and Architecture, Kore University of Enna, 94100 Enna, Italy

Corresponding authors: Taha A. Elwi (taelwi82@gmail.com), Mohammad Alibakhshikenari (mohammad.alibakhshikenari@uc3m.es), and Giovanni Pau (giovanni.pau@unikore.it)

Dr. Mohammad Alibakhshikenari acknowledges the support from the CONEX-Plus programme funded by Universidad Carlos III de Madrid and the European Union's Horizon 2020 research and innovation programme under the Marie Skłodowska-Curie grant agreement No. 801538. Additionally, the authors sincerely appreciate funding from Researchers Supporting Project number (RSP2024R58), King Saud University, Riyadh, Saudi Arabia.

**ABSTRACT** Rain attenuation poses a significant challenge for high-throughput communication systems. In response, this paper introduces an artificial intelligence (AI) model designed for predicting and mitigating rain-induced impairments in high-throughput satellite (HTS) to land channels. The model is based on three AI algorithms developed using 3D antenna design to characterize, analyze, and mitigate rain-induced attenuation, optimizing channel quality specifically in the United Arab Emirates (UAE). The study evaluates various parameters, including rain-specific attenuation, effective slant path through rain, rain-induced attenuation, signal carrier-to-noise ratio, and symbol error rate, for five conventional modulation schemes: Quadrature Phase-Shift Keying (QPSK), 8-Phase Shift Keying (8-PSK), 16-Quadrature Amplitude Modulation (16-QAM), 32-QAM, and 64-QAM. Additionally, the paper introduces a new database detailing rain-induced attenuation in HTS channels in the UAE at different frequencies using measured rainfall intensities. The paper concludes by proposing a smart antenna design with a frequency diversity technique for fade mitigation. Results indicate that rain-induced attenuation varies significantly based on rainfall rate and frequency. Specifically, at 25 GHz and a rainfall rate of 100 mm/h, the rain-induced attenuation can reach as high as 15 dB, resulting in a significant decline in signal quality and link performance. The

The associate editor coordinating the review of this manuscript and approving it for publication was Ravi Kumar Gangwar<sup>13</sup>.

proposed AI model demonstrates the ability to intelligently predict rain-induced attenuation and channel quality for various rainfall rates and frequencies. This information can be valuable for optimizing satellite link design and operation, ultimately enhancing the reliability and quality of satellite communications. The proposed two-slot smart antenna design utilizes frequency diversity to effectively mitigate rain attenuation, contributing to the overall improvement of link reliability and quality.

• **INDEX TERMS** Rain-induced attenuation, high throughput satellite (HTS), satellite communications, artificial intelligence (AI), UAE.

## I. INTRODUCTION

Modern satellite communication systems have sparked considerable interest in High Throughput Satellite (HTS) systems. These systems have become prominent for their ability to deliver efficient multimedia and broadband services at increased data rates, positioning them as focal points for the next generations of communication systems [1], [2], [3]. The demand for such HTS services has driven the need for more available bandwidth and higher data rates, leading to higher transmission frequencies [4]. Consequently, it has become imperative to characterize and model HTS channels at high frequencies to develop effective adaptive transmission models and mitigation techniques as solutions for channel impairments [4], [5]. To effectively meet user demands, it is crucial for these systems to operate at frequencies above 17 GHz [2], [3], [6].

Recent global advancements in satellite communication technologies have fueled a growing demand for advanced multimedia and broadband services provided by High Throughput Satellites (HTS) [7]. However, a major hurdle faced by HTS systems is the impact of rain-induced impairments on signal quality and link availability between HTS and terrestrial locations, especially at high frequencies [1], [8]. Raindrops act as obstacles, absorbing and scattering signal power, resulting in a degradation of signal quality as electromagnetic waves traverse through space [8], [9]. This degradation becomes more pronounced as transmission frequencies exceed 10 GHz, intensifying with higher transmission frequencies [9], [10].

To address this challenge, AI-based models offer a solution by efficiently predicting and mitigating rain attenuation in both satellite and terrestrial communication networks [11]. While widely accepted models for predicting rain attenuation have been established based on extensive observations and monitoring over the years, these models rely on information related to rainfall rates. This information can be sourced from rainfall measurement devices or predicted rainfall maps based on specific studies [12], [13]. However, it's important to note that models depending on predicted rainfall values may not always accurately forecast the performance of rain attenuation [8], [14], [15], [16], [17], [18], [19].

The accuracy of rain induced attenuation prediction models depends on the accuracy of the rainfall rate data used. Local rainfall rate measurements are preferred, especially with an integration time of at least 1-minute [15], [18], [20]. The ITU recommends using rain rate data for rain attenuation

prediction [19], [20], [21], [22], but this data can be difficult to obtain. Therefore, researchers are developing new prediction models with the use of actual measured rainfall rate [19].

Rain events, constituting only a small fraction of the year, typically occur less than 5% of the time. The International Telecommunication Union Radiocommunication Sector (ITU-R) has adopted this percentage as a starting point for their model. However, to accurately characterize rainy conditions globally, it is crucial to consider a percentage of less than 1% of the time in the year, as this period encompasses the rainfall that significantly impacts signal attenuation [23]. Specifically, heavy rain, which poses the most significant challenge, occurs in just 0.01% of the annual timeframe, resulting in severe signal quality degradation. Therefore, the 0.01% figure becomes particularly pertinent when analyzing the effects of heavy or highly effective rain attenuation [24].

The existence of channel impairments emphasizes the need for a channel model capable of predicting rain-induced attenuation and assessing signal quality to implement Fade Mitigation Techniques (FMT). The demand for high-speed data services in both developed and developing countries, coupled with the complex atmospheric dynamics in certain regions like the United Arab Emirates (UAE), is further compounded by the absence of a reliable prediction model for rain-induced effects on High Throughput Satellite (HTS) channels. Additionally, there's a scarcity of rain attenuation and mitigation models based on artificial intelligence (AI) specifically tailored for 5G and beyond communication links [11]. This underscores the importance of developing an AI model customized for the unique conditions of the UAE. Hence, addressing this issue involves designing an antenna that covers a wide range of frequencies to effectively mitigate the effects of channel impairments at different frequencies.

The high data rate of High Throughput Satellites (HTS) necessitates a robust signal strength with minimal transmission errors. Achieving this goal involves the development of an efficient and adaptive antenna design integrated with fade mitigation techniques. However, challenges arise from heavy rain impairments that degrade the quality of the satellite signal, leading to increased transmission errors. These errors can pose serious problems in receiving accurate and reliable data.

In response to these challenges, this paper presents the first HTS-to-land smart channel prediction model in the United Arab Emirates (UAE), utilizing a 3D slot array cone antenna

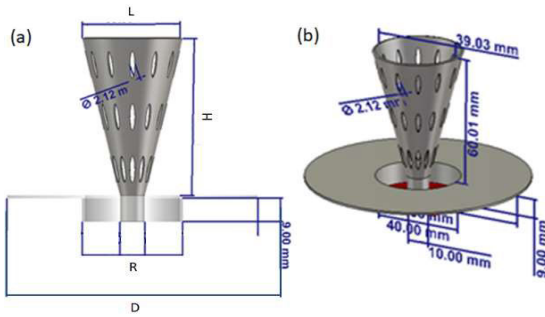


FIGURE 1. Antenna geometrical details.

TABLE 1. Dimensions of the proposed antenna element.

Parameters	Expression	Value (mm)
H	Cone height	60
L	Cone diameter	40
R	Feed aperture	40
D	Reflector diameter	100

to achieve a wideband with high gain across the entire frequency band of interest. The primary objective is to forecast the impact of rain-induced impairments and assess channel quality at the K and Ka frequency bands. Real measured rain-fall data is employed with the proposed antenna, which boasts a high gain bandwidth product. Remarkably, the influence of rain on satellite communication channels in the UAE has remained largely unexplored in prior research, as far as the authors are aware. This study seeks to bridge this gap by offering valuable insights into the complexities of rain effects on HTS systems. Additionally, it proposes an innovative slot array antenna design to mitigate these effects and enhance overall channel performance.

## II. ANTENNA GEOMETRICAL AND DETAILS

This section provides an explanation of the geometrical details of the antenna, with dimensions presented in millimeter scale as illustrated in Fig. 1. The proposed antenna is specifically designed to function as a high-gain end-fire antenna. In this design, a circular cross-sectional cut cone is employed to smoothly guide the wave between the microwave source and the free space impedance [25]. To further enhance performance, elliptical slots are incorporated into the cone design to reduce tangential surface waves and concentrate the main beam onto the sight bore direction [26].

Activation of the antenna involves two microwave ports positioned horizontally and vertically, with a 90° phase shift to induce circular motion along the antenna’s transverse axial. To maintain directivity in the main lobe direction and increase the front-to-back ratio, a circular ground plane reflector supports the antenna [27]. The entire antenna structure measures 70 × 100 × 100 mm<sup>3</sup> and is constructed from Aluminum in a 3D form, as depicted in Fig. 1. Additional dimensions for the proposed antenna are detailed in Table 1. For consistent microwave feeding across a wide range of frequencies, the antenna is connected through SMA type connectors.

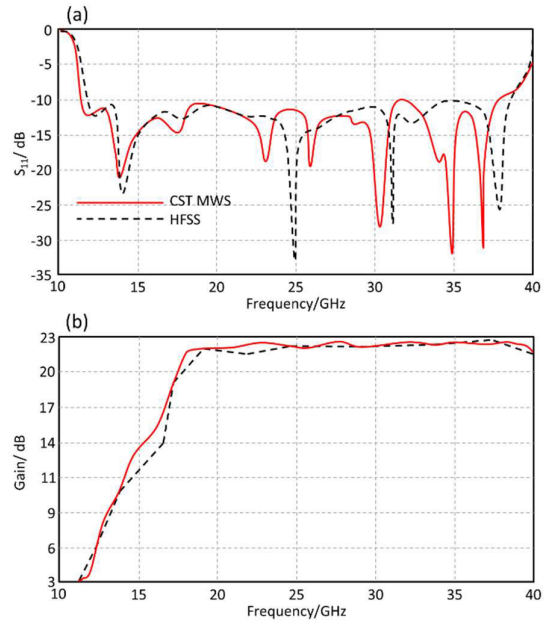


FIGURE 2. Antenna performance validation: (a)  $S_{11}$  response, and (b) gain response.

The antenna design underwent optimization through CST and HFSS 3D electromagnetic field solvers. To assess its performance, the proposed antenna’s  $S_{11}$  and gain spectra were compared with measured results, revealing excellent agreement between simulation and measurement, as depicted in Fig. 2. Over the frequency range of 18 GHz to 40 GHz, the proposed antenna exhibits a gain of 22 dBi, accompanied by an outstanding match impedance of less than  $-10$  dB.

Measurements indicate that the effects of rain between 18 GHz to 40 GHz can be mitigated by smoothly changing the frequency carrier during operation. This broad frequency bandwidth is achieved by incorporating an array of slots on the cone antenna, effectively suppressing surface waves, and positively impacting the impedance bandwidth of the antenna [28]. Furthermore, the directivity of the antenna is enhanced through the integration of a circular reflector at the base, positioned next to the input feed, as illustrated in Fig. 1. This reflector significantly suppresses side lobes, contributing to an overall improvement in antenna performance [29].

The proposed antenna exhibits an impressive gain bandwidth product, primarily attributed to the tangential traveling wave phenomena [30]. The axial-ratio (AR) of the antenna is illustrated in Fig. 3(a). Specifically, the AR of the proposed antenna measures approximately 3 dB at both 20 GHz and 30 GHz, which are the frequency bands of interest. Fig. 3(b) displays the radiation patterns of the antenna at 20 GHz and 30 GHz in both the E-plane and H-plane. Notably, the antenna exhibits an end-fire radiation pattern, a characteristic attributed to the effects of the antenna reflector, which contributes to achieving high normalization in the E-plane [31].

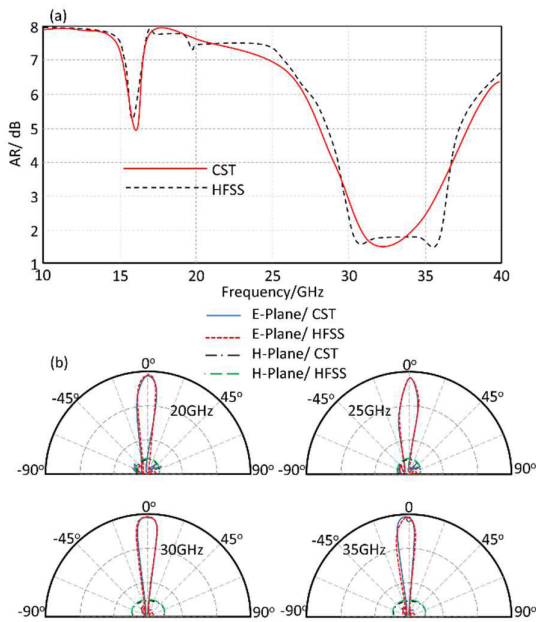


FIGURE 3. Antenna radiation properties: (a) AR, and (b) radiation patterns at 20 GHz, 31 GHz, 20 GHz, and 30 GHz.

### III. EXPERIMENTAL VALIDATION AND DISCUSSION

The proposed antenna was manufactured using 3D printing technology, employing PLA (Polylactic Acid) material for its convenience and cost-effectiveness [28]. Specifically, the 3D printing technology utilized was based on Fused Deposition Modeling (FDM), known for its excellent printing precision [29]. This FDM technology operates by “slicing” the 3D model into thin horizontal layers, which are then printed on top of each other to construct the entire structure. This process generates a G-code file containing instructions for the printer. Subsequently, these G-code instructions are executed to systematically build the object layer by layer along the x, y, and z axes, with the filament being extruded through a heated nozzle onto the print bed.

The fabricated antenna was then coated with a conductive aluminum layer. To ensure a proper power match, it was fed through an SMA port. The antenna’s radiation characteristics were measured within an RF anechoic chamber, as illustrated in Fig. 4, using a standard measurement setup. Notably, the reflector part of the antenna was connected to the SMA ground plane.

A comparative analysis of the proposed antenna’s characteristics against other recently published works is presented in Table 2. The results reveal that the proposed antenna exhibits an outstanding gain bandwidth product when compared to findings in the existing literature, all within a sufficiently miniaturized size.

Millimeter waves find diverse applications, such as wireless communication, detection, and remote sensing [32]. However, signals operating in the millimeter wave range are significantly attenuated by the atmosphere [33]. To address this attenuation, the use of a high-gain antenna becomes

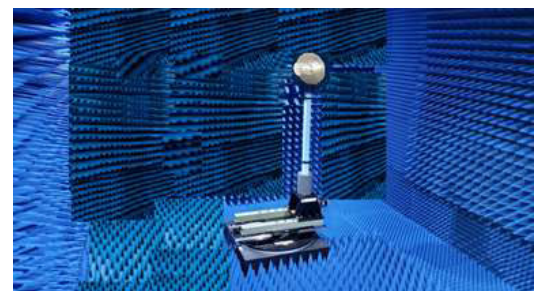


FIGURE 4. Fabricated antenna design.

TABLE 2. Antenna performance comparison with published works in literature.

Ref.	Antenna size (mm <sup>3</sup> )	Type	BW (GHz)	Gain (dBi)	Applications
[32]	15.2×16.5×1.6	Microstrip	35-40	-----	Glucose sensing
[33]	6.25×6.25×1.7	Microstrip	30	-----	Food sensing
[34]	400×200×2	Horn	32-38	12	Rader detection
[35]	100×100×1.4	Horn	100-300	-----	Remote sensing
[36]	250×250×2.1	Horn	26-60	12	Land mine detection
[37]	2.8×2.4×1.7	Microstrip	28-160	1.5-7	5G
[38]	3.5×3.5×1.2	Microstrip	38	-----	Comms.
This work	90×100×100	3D slot array	1-30	3-22.5	Comms.

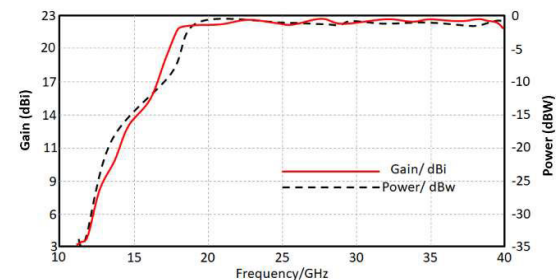


FIGURE 5. The proposed antenna performance in terms of gain and power spectra.

crucial. Our study specifically explores how gain is affected as a function of frequency in a free space environment, with

the transmitter positioned 10 meters away from the receiver. Fig. 5 illustrates the variations in power and gain for the proposed antenna. Notably, the antenna achieves a gain of approximately 21.5 dBi at 31 GHz with a power level of  $-1.2$  dBw.

In the context of wireless communications, fundamental concepts include path loss and fading effects. Attenuation, a critical aspect in wireless communication systems, denotes the reduction of signal power or energy as it traverses through a medium like air, water, or solid objects. Path loss, on the other hand, refers to the decline in signal power over distance in free space without obstacles or interference. Fading encompasses variations in signal strength during propagation due to interference, reflections, and scattering.

Fading effects can lead to fluctuations in received signal strength over time, resulting in signal degradation and diminished communication performance. Two primary types of fading exist: slow fading, occurring over extended periods due to environmental changes like rainfall or cloud accumulation, and fast fading, transpiring over short intervals due to multipath propagation and rain-induced tropospheric scintillation. Fast fading involves reflections and scattering, causing constructive or destructive interference at the receiver.

Various factors influence the extent of impairments, including rain parameters (rain height, rainfall rate) and transmission parameters (frequency, modulation scheme). Frequency ( $f$ ) plays a crucial role, as per the Friis transmission equation, where it is directly proportional to signal power attenuation and, consequently, the Signal-to-Noise Ratio (SNR), potentially leading to increased error rates. For frequencies below 3 GHz, ionospheric scintillation significantly affects, while frequencies above 10 GHz see substantial impact from atmospheric phenomena like rain and clouds [41].

#### IV. RAINFALL CHARACTERISTICS IN UAE

The Middle East, situated on the northeastern edge of the Arabian Peninsula, covers an area of approximately 83,600 km<sup>2</sup> [42]. Comprising seven emirates, most of which border the northeastern shores of a gulf (depicted in Fig. 6), the United Arab Emirates (UAE) straddles the boundary between tropical and subtropical climates. The UAE's climate is characterized by two primary regions: a vast desert dominating the central and western parts of the country, resulting in desert-like climate attributes, and the northeastern border along the Gulf, where the presence of the sea contributes to higher humidity levels [43]. The subsidence of air in this region leads to a significant rise in average annual temperatures during the summer, making this area one of the hottest on the planet. Consequently, most rainfall in the UAE is concentrated between November and March [43].

Merabtene et al. [44] conducted extensive rainfall rate measurements in the UAE spanning over 80 years (1934 to 2014) to determine the average annual rainfall rate. However, notable changes in rainfall characteristics, especially after 1998 [45], [46], prompted a focus on measurements

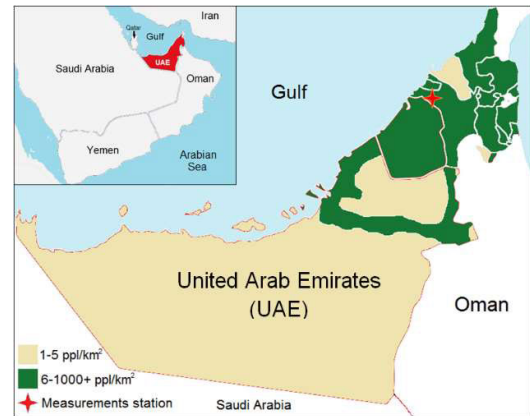


FIGURE 6. UAE map with measurements of the station location.

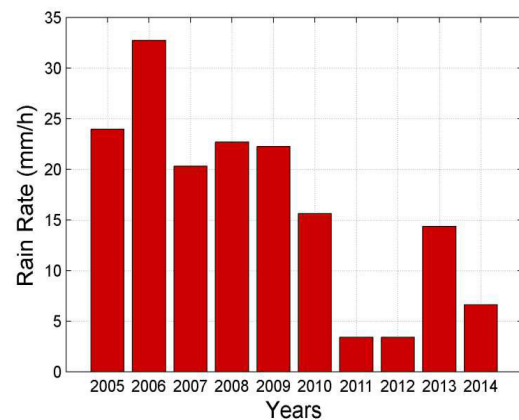


FIGURE 7. Average measured rainfall rates.

post-1998, reflecting the rain-induced impairments experienced in the UAE. Examining weather effects on satellite channels and service quality is crucial, particularly in the northeastern region where much of the population resides (as depicted in Fig. 6).

Rainfall in the UAE primarily occurs during the winter months and typically registers below 100 millimeters. Precipitation events manifest as showers, heavy rainfall, and, at times, extreme rainfall, particularly in densely populated areas like Dubai and Sharjah [44]. To capture regional nuances, rainfall rates have been closely monitored in the northeastern region, including the installation of a tipping bucket rain gauge at Sharjah International Airport. Accurate annual rainfall data is essential [20], [47], [48]. Over a ten-year period (2005 to 2014), average rainfall rates were meticulously measured and recorded, as illustrated in Fig. 7.

Data for this analysis was sourced from the Meteorological office at Sharjah International Airport [44]. Initial measurements were in millimeters and later converted to millimeters per hour (mm/h). During this decade-long observation, the maximum recorded rainfall rate was 33 mm/h in 2006, while the minimum rate of 4 mm/h occurred during the drier years of 2011 and 2012. The average measured rainfall rate over this ten-year period was determined to be 16.5 mm/h,

enhancing the accuracy of rainfall rate performance characterization for the region [47], [48].

## V. PROPOSED PREDICTION MODEL OF THE RAIN IMPAIRMENTS AND CHANNEL QUALITY

This section introduces a novel model for predicting rain-induced impairments and assessing channel quality for the HTS-to-land communication channel in the UAE. The experimental setup to validate the proposed model consisted of multiple line-of-sight terrestrial links, with both the transmitter and receiver mounted on an aluminum pipe at a height of 7 meters above the ground. Each link was positioned 2.8 km apart. The transmission involved modulated signals within a carrier frequency range of 18 GHz to 40 GHz, and the maximum transmit power was set at +30 dBm. Signal levels were measured with a scalar network analyzer at 10-second intervals and systematically recorded using a data logger. To capture real-time environmental conditions, on-site rain gauges were deployed to measure the actual rainfall rate throughout the experiment.

The model consists of three algorithms designed to enhance prediction accuracy and improve overall signal quality assessment.

**Algorithm 1** focuses on predicting rain attenuation over a 1 km slant path. It utilizes a modified ITU-R prediction model [23] and incorporates a novel approach called the Attenuation-Specific Data Mining (ASDM) procedure. The key innovation is the use of actual measured rainfall rate data [13], replacing the predicted values from the ITU. This substantial improvement in data accuracy results in more precise predictions of rain-specific attenuation [49] and, subsequently, HTS-to-land signal quality.

**Algorithm 2** addresses the effective slant path length, adapting it based on horizontal projection adjustments and vertical length modifications, considering the specific meteorological data in the UAE [16], especially related to rain in the troposphere.

**Algorithm 3** further refines the model by AI-based predicting rain-induced attenuation and its impact on HTS channel quality. It specifically evaluates the carrier-to-noise ratio and symbol error rate for five commonly used modulation schemes (QPSK, 8PSK, 16-QAM, 32-QAM, and 64-QAM). Algorithms 1 and 2 serve as the foundational input for the calculations in this algorithm. These modulation schemes were used in the single-media or multimedia communication standards like Digital Video Broadcasting via Satellite (DVB-S) and Digital Video Broadcasting via Satellite-Second Generation (DVB-S2) and (DVB-S2X) which are mostly employed worldwide [24], [50], especially in the middle-eastern countries.

Algorithm 1 calculates the rain-specific attenuation, a critical parameter for precise rain attenuation predictions [51]. This attenuation represents the electromagnetic power absorbed and scattered by rain droplets over a 1 km path, directly influenced by the transmission frequency. The coefficients, denoted as 'k' and ' $\alpha$ ', vary based on

**TABLE 3. Conventional telecommunication parameters.**

Parameter	Value
EIRP	68.5 dB
$G_r$	55 dBi
$R_S$	30 Msps
$\theta$	45°
$h_S$	6m above sea level
$L_{sys}$	1 dB

factors like droplet size distribution, frequency, and electromagnetic wave polarization. Algorithm 2 accounts for the inhomogeneity of rain in both vertical and horizontal directions, introducing factors such as the Vertical Adjustment Factor (VAF) and Horizontal Reduction Factor (HRF) to consider temporal variations in raindrop dimensions and rain height [16]. The calculation of these factors relies on a high rainy percentage (0.01%) of annual time, reflecting the temporal variability of rain-related dimensions. To estimate the non-homogeneity of rain along the propagation path, Algorithm 2 incorporates the effective path length ( $L_E$ ).

The two algorithms are validated for different locations in the middle east [8], [52] and found to have a prominent accuracy, then - in this study - the developed Algorithm 3 is attached to algorithms 1 and 2 for the design of comprehensive channel analysis model in UAE and acquiring precise channel state information for optimizing proper fade mitigation technique by integrating a frequency diversity aware-antenna design.

The results obtained from Algorithms 1 and 2 serve as the input parameters for Algorithm 3, allowing for the prediction of rain-induced signal loss in the HTS system, with measurements given in dB/km and the effective slant path length in kilometers. A summary of the telecommunication parameters for the three algorithms is provided in Table 3, including actual measured values. Algorithm 3 is instrumental in estimating, evaluating, and analyzing the link availability and signal quality of the HTS-to-land communication channel under rainy conditions. It offers insights into long-term statistics related to rain-induced attenuation, assesses link margin through carrier-to-noise ratio, and analyzes the overall reduction in received power. The Free Space Loss (FSL) is assessed based on the transmitted frequency and link distance (d) to gauge HTS communication service quality. The subsequent analysis involves evaluating quality performance in the UAE, particularly in terms of the Symbol Error Rate (SER), which serves as a quality indicator. SER is theoretically estimated using three conventional modulation schemes frequently employed in satellite communication systems: QPSK, 8-PSK, 16-QAM, 32-QAM, and 64-QAM. This comprehensive model empowers the selection of an optimal Fade Mitigation Technique (FMT) to maintain reliable communication during rainy conditions.

## VI. DISCUSSION

To detect the impact of rain-induced impairments on the HTS-to-land channel, the elevation angle is settled to a fixed value

<p><b>Algorithm1:</b></p> <ol style="list-style-type: none"> <li>1. Input transmission-specific parameters (elevation angle <math>\theta</math>, frequency <math>f</math>, and polarization angle <math>\tau</math>).</li> <li>2. Input actual measured rainfall rate data in millimeters (mm) and convert the average rainfall rate data on a given time interval of 1 min to mm/h.</li> <li>3. Obtain frequency-dependent coefficients <math>k</math> and <math>\alpha</math> [3]:           <math display="block">k = \frac{k_H + k_V + (k_H - k_V) \cos^2 \theta \cos(2\tau)}{2}</math> <math display="block">\alpha = \frac{k_H \alpha_H + k_V \alpha_V + (k_H \alpha_H - k_V \alpha_V) \cos^2 \theta \cos(2\tau)}{2k}</math>           Where the empirical values related to the horizontal polarization (<math>k_H</math> and <math>\alpha_H</math>) and vertical polarisation (<math>k_V</math> and <math>\alpha_V</math>) are obtained from [53].         </li> <li>4. Calculate the rain-specific attenuation (rain-induced attenuation for 1 km slant path) using 1-min cumulative distribution rainfall rate expressed in (dB/km) [3]: <math>\gamma_{Rain} = \alpha(R)^k</math></li> </ol>	
<p><b>Algorithm2</b></p> <ol style="list-style-type: none"> <li>1. Input earth station-specific parameters (latitude <math>\phi</math>, longitude <math>L</math>, station height <math>h_s</math>, elevation angle <math>\theta</math>).</li> <li>2. Input transmission-specific parameters (frequency <math>f</math>, and polarization angle <math>\tau</math>).</li> <li>3. Obtain zero isotherm height <math>h_0</math> in UAE from ITU recommendation [54].</li> <li>4. Determine the rain height [54], [55]:           <math display="block">h_R = h_0 + 0.36</math> </li> <li>5. Calculate the actual slant path length <math>L_S</math> [23]:            if <math>\theta \geq 5^\circ</math>, then <math>L_S = \frac{h_R - h_S}{\sin \theta}</math>            otherwise,           <math display="block">A = \pi r^2 L_S = \frac{2(h_R - h_S)}{\sqrt{\sin^2 \theta + \frac{2(h_R - h_S)}{E_{ER}} + \sin \theta}}</math>           Where the earth's equivalent radius <math>E_{ER} = 4r_e/3</math> and <math>r_e</math> is the earth's radius in km.         </li> <li>6. Obtain the slant path horizontal projection.           <math display="block">P_H = L_S \cos \theta</math> </li> <li>7. Estimate the horizontal reduction factor HRF:           <math display="block">HRF = \frac{1}{1 + 0.78 \sqrt{\frac{P_H \gamma_R}{f} - 0.38 (1 - e^{-2P_H})}}</math> </li> <li>8. Calculate the adjusted elevation angle <math>\xi</math> based on planner geometry.           <math display="block">\xi = \tan^{-1} \left( \frac{h_R - h_S}{P_H HRF} \right)</math> </li> <li>9. Estimate the effective slant path through the rain <math>L_R</math>:            if <math>\xi &gt; \theta</math>, then <math>L_R = \frac{P_H r_H}{\cos \theta}</math>            otherwise, <math>L_R = \frac{H_R - H_S}{\sin \theta}</math>            Estimate the vertical adjustment factor VAF:           <math display="block">VAF = \frac{1}{1 + \sqrt{\sin \theta} \left[ 31 \left( 1 - e^{-\frac{\theta}{1-\chi}} \right) \frac{\sqrt{L_R \gamma_R}}{f^2} - 0.45 \right]}</math> </li> <li>10. Calculate the effective slant path length <math>L_E</math>:           <math display="block">L_E = L_R V_F</math> </li> </ol>	<p><b>Algorithm 3</b></p> <ol style="list-style-type: none"> <li>1. Input the telecommunication parameters.</li> <li>2. From the results of Algorithms 1 and 2, calculate the predicted attenuation exceeded 0.01% of an average year:           <math display="block">A_{0.01} = \gamma_{Rain} L_E</math> </li> <li>3. Calculate the coefficient function <math>\beta</math> of the percentage of time [23].            if <math>p \geq 1</math> or <math> \lambda  \geq 36^\circ</math> or, then <math>\beta = 0</math>            if <math>p &lt; 1</math>, and <math> \lambda  &lt; 36^\circ</math>, then <math>\beta = 0.005 ( \lambda  - 36)</math>            otherwise, <math>\beta = 0.005 ( \lambda  - 36) + 1.8 - 4.25 \sin \theta</math> </li> <li>4. Predict the rain-induced loss at all rainy percentages of time:           <math display="block">L_{rain} = A_{0.01} \left( \frac{p}{0.01} \right)^{-F_p}</math>           Where  <math display="block">F_p = 0.655 + 0.033 \ln(p) - 0.045 \ln(A_{0.01}) - \beta(1-p) \sin \theta</math> </li> <li>5. Calculate the losses in free space (non-rainy environment)           <math display="block">L_{FS} = 20 \log \left( \frac{4\pi d}{\lambda} \right)</math>           Where <math>d</math> is the link distance, and <math>\lambda</math> is the signal wavelength.         </li> <li>6. Calculate the carrier-to-noise ratio in dB:           <math display="block">CNR = EIRP + G_r - L_{FS} - L_{rain} - L_{sys} - N</math>           Where <math>EIRP</math> is the effective isotropic radiated power, <math>G_r</math> is the receiver gain, <math>L_{sys}</math> is the system loss, and <math>N</math> is the noise that depends on the noise temperature and bandwidth.         </li> <li>7. Calculate the symbol energy to noise ratio:           <math display="block">E_S/N = CNR + 10 \log \left( \frac{BW}{R_S} \right)</math>           Where <math>BW</math> is the signal bandwidth, and <math>R_S</math> is the symbol rate.         </li> <li>8. Estimate the symbol error rate <math>SE_R P_{se}(E_S/N)</math> for 5 modulation schemes. [56], [57].</li> </ol>

due to its effective role on the rain attenuation value. The rain-induced attenuation is extracted for 10 years in UAE based on the proposed prediction model that considered the

effective rainy conditions for a period of 10 years, as shown in Figs. 8 and 9. By calculating the mean rain-induced attenuation, the resultant prediction data is evaluated to realize a

unique performance for the UAE satellite channel at the K and Ka bands, as listed in Table 4, where the presented database of the rain-induced losses of the UAE satellite channel is exhibited from 18 GHz to 40 GHz frequencies for different rainfall intensities. Fig. 8 shows that the UAE in 2006 had the highest rain attenuation of 24 dB for the 0.01% of the annual period when the frequency of the transmitted satellite signal equals 20 GHz. This is due to a much higher rain rate that reached 33 mm/h. The channel attenuation performance decreased for the years 2005, 2007, 2008, and 2009 to be bound between 16 dB and 18 dB because the rainfall rates in those years were between 21 mm/hr and 24 mm/hr. Whereas the predicted rain attenuation in the dry years of 2011 and 2012 is approximately 4 dB and is raised to 6 dB in 2014.

It is known that the UAE shares borders with the gulf from the north side and contains a vast desert that dominates 70% of the entire country on the east-western side [58], affecting the nature and direction of the monsoon. Consequently, unique atmospheric parameters are introduced. The intense rainfall rate times happen in 0.001% of the year, roughly the highest 9 hours/year rainfall rate. At these times, the induced loss increased significantly to reach approximately 42 dB in 2006 and 29 dB to 33 dB in the years 2005, 2007, 2008, and 2009. To a lesser extent, the rain attenuation reaches lower levels at the rest of the period of interest, which reflects the lower and normal rainfall rate in the UAE. The value of the rain-induced loss increases with the increase of the transmission frequency. The plot of rain-induced loss of HTS signal at higher frequencies can visualize the effect of transmission frequency. The predicted rain-induced loss values at 30 GHz are shown in Fig. 9 for the period of 10 years. At present, 20 and 30 GHz are the usual frequencies for transmitting data to and from satellite systems, respectively. Fig. 9 demonstrates that in the rainiest year of 2006, there was a rain attenuation of up to 50 dB 0.01% of the time. The values of rain-induced attenuation were between 34 dB and 39 dB in the wet years 2005–2009 at 30 GHz. However, it was discovered that the rainfall rate was extremely high, resulting in rain attenuation of up to 82 dB at 0.001% of the time in 2006. In contrast, the dry sky of 2011 and 2012 had rain attenuation limited to 16 dB. This could pose a severe risk to the satellite link's availability. The connection of an earth station to a different satellite led to a variation in the rain attenuation due to an alteration in the elevation angle  $\theta$ . Moreover, the present study investigated the effect of changes in elevation angle on the rain attenuation prediction in the UAE, even when the earth station is connected to the same satellite. Figs 10 and 11 depicted the impact of different elevation angles on rain-induced attenuation prediction in the UAE.

Figs. 10 and 11 illustrate that the rain induced attenuation increases as the angle of elevation decreases. It has been observed that, when operating at 20 GHz with an elevation angle varying from  $80^\circ$  to  $20^\circ$ , the signal attenuation at 0.01% of the time is in the range of 11 dB to 25 dB because of the increase in the slant path length, thus requiring the

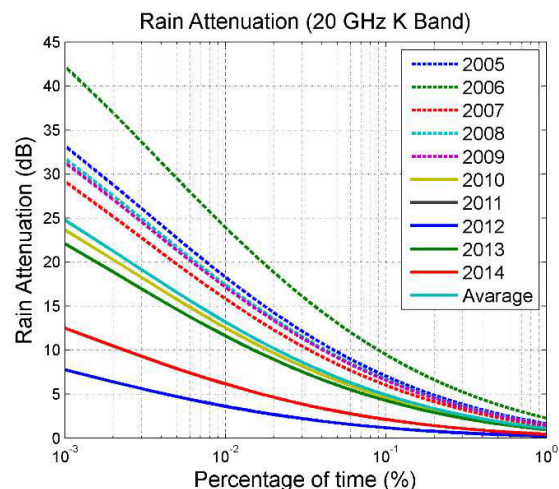


FIGURE 8. Rain induced attenuation at 20 GHz.

signal to traverse a higher significant number of rain droplets. In contrast, the elevation angle varies from  $21^\circ$  to  $35^\circ$  dB for the most extreme rainfall rates of 0.001% of the year. At 30 GHz, the rain induced effects on satellite link become relatively higher. The rain attenuation reaches 52 and 68 dB for elevation angle of  $20^\circ$  at heavy and extreme rainfall rate periods, respectively. Whereas for a high elevation angle,  $80^\circ$ , the attenuation reaches 40 dB at extreme rainfall rate and 24 dB at heavy rainfall rate at 0.01% of time. Moreover, as the elevation angles increased, the convergence of the attenuation performances increased simultaneously. This high difference in rain-induced attenuation between the low and high elevation angles reflects the paramount consideration that should be considered in the design of the HTS-to-land channel and the need for implementing the proposed model.

As the intensity of the rainfall increased, there was a notable diminishment in the signal strength, which can be best expressed as a signal carrier-to-noise ratio CNR [59]. Since the proposed antenna covers a wide range of frequencies with a stable gain, the authors conducted an experiment to switch the frequency of operation from 20 GHz to 30 GHz to realize the effects of that on the CNR as Fig. 12. It is obvious the value of the evaluated CNR at 20 GHz, in general is higher than the one at 30 GHz. Therefore, to mitigate the effects of rain, using the communication link at 20 GHz is more feasible.

The impact of rain on satellite signals is evident, particularly affecting the received signal level and, consequently, the Carrier-to-Noise Ratio (CNR), especially at higher rainfall rates. At a frequency of 20 GHz, rain-induced impairments can reach approximately 18 dB for heavy rainfall and up to 30 dB for extreme rainfall rates. Notably, link availability becomes nonexistent at 30 GHz during periods of high rainfall rates. This underscores the necessity for implementing Fade Mitigation Techniques (FMT), as depicted in Fig. 12, but such implementation is required for less than 0.1% of the rainfall time.



**TABLE 4.** Proposed database of rain-induced loss on a satellite channel in UAE for an average of 10 years.

Frequency (GHz)	Rain-induced loss (dB)		
	Moderate rainfall p=0.1%	Heavy rainfall p=0.01%	Extreme rainfall p=0.001%
18	3.9	10.7	20.4
19	4.4	11.9	22.6
20	4.9	13.2	24.7
21	5.5	14.5	27.0
22	6.0	15.9	29.3
23	6.6	17.4	31.7
24	7.3	18.8	34.1
25	7.9	20.4	36.5
26	8.6	21.9	39.0
27	9.3	23.5	41.6
28	10.0	25.1	44.1
29	10.7	26.8	46.7
30	11.5	28.4	49.3
31	12.2	30.1	51.9
32	13.0	31.8	54.5
33	13.7	33.5	57.0
34	14.5	35.2	59.6
35	15.3	36.8	62.1
36	16.0	38.5	64.6
37	16.8	40.1	67.1
38	17.5	41.8	69.6
39	18.3	43.4	72.0
40	19.0	45.0	74.4

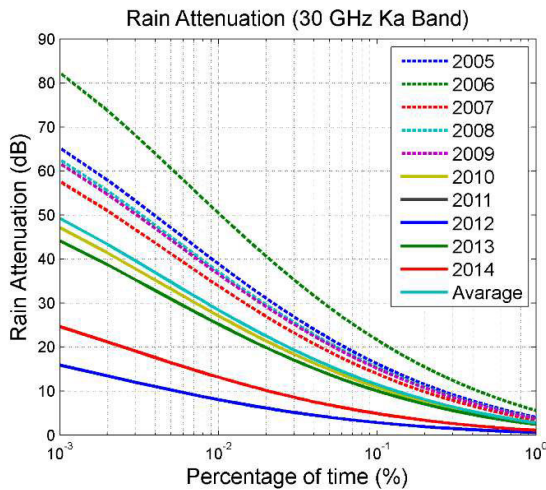


**FIGURE 9.** Rain induced attenuation at 30 GHz.

Additionally, rain significantly influences transmission error rates. With an increase in the rainfall rate, the Symbol Error Rate (SER) rises simultaneously. Assuming no error correction is applied, the rain-induced SER on the HTS-to-land signal is evaluated for three conventional modulation schemes, as illustrated in Fig. 13. Both the transmission frequency and the type of modulation scheme exert substantial impacts on SER. Specifically, the SER reaches 0.9 at the extreme rainfall rate, occurring in 0.001% of time, for the highest (64-QAM) modulation scheme. In contrast, the SER is relatively lower for lower M-ary modulation schemes, reaching SER values of 0.59, 0.27, and 0.1 for 32-QAM, 16-QAM, and 8-PSK, respectively, under extremely high rainfall rates. For QPSK, the rain-induced SER at 20 GHz has

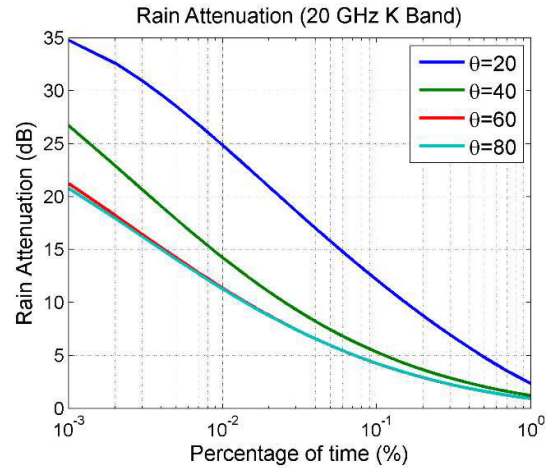


**FIGURE 10.** Rain induced attenuation for different  $\theta$  at 20 GHz.

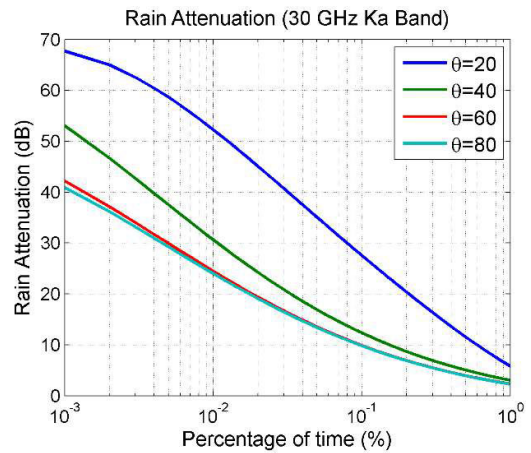


**FIGURE 11.** Rain induced attenuation for different  $\theta$  at 30 GHz.

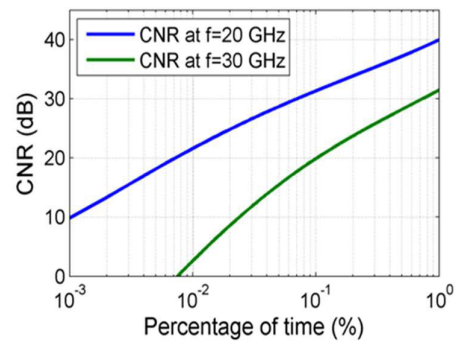


**FIGURE 12.** Carrier-to-noise ratio for different transmission frequencies as a function of rainfall percentage of time.

a negligible effect but exponentially increases for less than 0.001% of time under extreme rainfall rates.

UAE has a relatively low rainfall rate compared to most tropical countries that experience a severe problem of rainfall events at the K and Ka frequency bands. However, under extreme rainfall conditions it is recommended that FMT such as frequency diversity be employed.

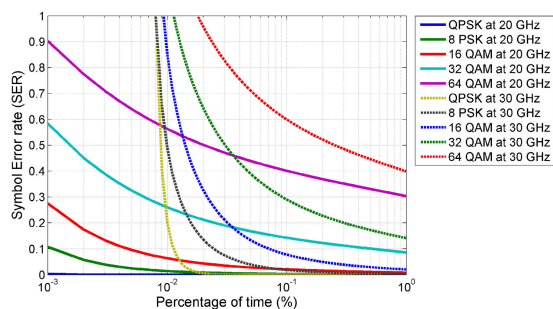


**FIGURE 13.** Symbol error rate for different frequencies and modulation schemes.

## VII. CONCLUSION

The AI prediction and mitigation of rain-induced attenuation play a crucial role in establishing effective high-throughput satellite (HTS) communication links, especially at frequencies exceeding 17 GHz. This study offers the inaugural estimate and forecast of link-level availability for HTS in the UAE, utilizing channel quality. It proposes an AI-based frequency diversity antenna model as a fade mitigation technique. Using actual rainfall rate data, the model incorporates three AI algorithms to determine rain-induced fade levels, Carrier-to-Noise Ratio (CNR), Energy per Symbol to Noise Power Spectral Density Ratio ( $E_s/N$ ), and the probability of symbol errors for five modulation schemes. Covering a decade of channel measurements, the study presents the average rain-induced fade level and creates a detailed database of losses at various frequencies and rainfall intensities. The analysis of rainfall impact on HTS links in the UAE, considering different transmission frequencies and elevation angles, reveals the significant influence of elevation angles on link quality. Transmission frequency proves notably effective during intense rainfall, affecting link availability at higher modulation schemes. The study recommends employing the proposed model during rainfall events for enhanced HTS channel quality, suggesting its adoption by system designers and channel providers in the UAE. Furthermore, the paper introduces a prediction model for rain-induced attenuation and channel quality in the high-throughput satellite channel in the UAE. Validation results affirm the model's effectiveness in predicting rain attenuation impacts on satellite link performance, providing accurate channel quality predictions to optimize satellite link design and operation. The research contributes valuable insights to satellite communications, emphasizing the proposed antenna's feasibility in mitigating rain effects by allowing a seamless frequency switch within a broad bandwidth from 12 GHz to 40 GHz, maintaining stable gain around 22 dBi. Extension of this research is suggested to include other modulation schemes, covering diverse geographic locations, and conducting experimental measurements of satellite signal attenuation during rainy environment to robustly validate the rain induced attenuation analysis and prediction.

## REFERENCES

- [1] R. De Gaudenzi, P. Angeletti, D. Petrolati, and E. Re, "Future technologies for very high throughput satellite systems," *Int. J. Satell. Commun. Netw.*, vol. 38, no. 2, pp. 141–161, Mar. 2020.
- [2] K. Kaneko, H. Nishiyama, N. Kato, A. Miura, and M. Toyoshima, "Construction of a flexibility analysis model for flexible high-throughput satellite communication systems with a digital channelizer," *IEEE Trans. Veh. Technol.*, vol. 67, no. 3, pp. 2097–2107, Mar. 2018.
- [3] L. Ippolito, *Satellite Communications Systems Engineering: Atmospheric Effects, Satellite Link Design and System Performance*. Wiley, 2017, p. 464.
- [4] S. Scalise, H. Ernst, and G. Harles, "Measurement and modeling of the land mobile satellite channel at Ku-band," *IEEE Trans. Veh. Technol.*, vol. 57, no. 2, pp. 693–703, Mar. 2008.
- [5] A. Abdi, W. C. Lau, M. Alouini, and M. Kaveh, "A new simple model for land mobile satellite channels: First- and second-order statistics," *IEEE Trans. Wireless Commun.*, vol. 2, no. 3, pp. 519–528, May 2003.
- [6] R. Zhang, Y. Ruan, Y. Li, and C. Liu, "Interference-aware radio resource management for cognitive high-throughput satellite systems," *Sensors*, vol. 20, no. 1, p. 197, Dec. 2019.
- [7] (2020). *Space Science and Technology—The Official Portal of the UAE Government*. [Online]. Available: <https://u.ae/en/about-the-uae/science-and-technology/key-sectors-in-science-and-technology/space-science-and-technology>
- [8] A. M. Al-Saegh and T. A. Elwi, "Direct extraction of rain-induced impairments on satellite communication channel in subtropical climate at K and Ka bands," *Telecommun. Syst.*, vol. 74, no. 1, pp. 15–25, May 2020.
- [9] A. M. Al-Saegh, A. Sali, J. S. Mandeep, and F. Pérez Fontán, "Channel measurements, characterization, and modeling for land mobile satellite terminals in tropical regions at Ku-band," *IEEE Trans. Veh. Technol.*, vol. 66, no. 2, pp. 897–911, Feb. 2017.
- [10] A. Z. Papafragkakis, C. I. Kouroriorgas, and A. D. Panagopoulos, "Performance of micro-scale transmission & reception diversity schemes in high throughput satellite communication networks," *Electronics*, vol. 10, no. 17, p. 2073, Aug. 2021.
- [11] E. Alozie, A. Abdulkarim, I. Abdullahi, A. D. Usman, N. Faruk, I.-F.-Y. Olayinka, K. S. Adewole, A. A. Oloyede, H. Chiroma, O. A. Sowande, L. A. Olawoyin, S. Garba, A. L. Imoize, A. Musa, Y. A. Adediran, and L. S. Taura, "A review on rain signal attenuation modeling, analysis and validation techniques: Advances, challenges and future direction," *Sustainability*, vol. 14, no. 18, p. 11744, Sep. 2022.
- [12] R. Crane, "Prediction of attenuation by rain," *IEEE Trans. Commun.*, vol. C-28, no. 9, pp. 1717–1733, Sep. 1980.
- [13] *Characteristics of Precipitation for Propagation Modelling*, document ITU-R P.837, International Telecommunication Union, Recommendation, 2017.
- [14] J. S. Mandeep, S. I. S. Hassan, and K. Tanaka, "Rainfall measurements at Ku-band satellite link in Penang, Malaysia," *IET Microw., Antennas Propag.*, vol. 2, no. 2, pp. 147–151, Mar. 2008.
- [15] J. S. Ojo, M. O. Ajewole, and S. K. Sarkar, "Rain rate and rain attenuation prediction for satellite communication in Ku and Ka bands over Nigeria," *Prog. Electromagn. Res. B*, vol. 5, pp. 207–223, 2008.
- [16] A. Adhikari, S. Das, A. Bhattacharya, and A. Maitra, "Improving rain attenuation estimation: Modelling of effective path length using Ku-band measurements at a tropical location," *Prog. Electromagn. Res. B*, vol. 34, pp. 173–186, 2011.
- [17] K. Badron, A. F. Ismail, J. Din, and A. R. Tharek, "Rain induced attenuation studies for V-band satellite communication in tropical region," *J. Atmos. Solar-Terrestrial Phys.*, vol. 73, nos. 5–6, pp. 601–610, Apr. 2011.
- [18] J. S. Mandeep, S. I. S. Hassan, and M. F. Ain, "Rain rate conversion for various integration time for equatorial and tropical climates," *Int. J. Satell. Commun. Netw.*, vol. 26, no. 4, pp. 329–345, Jul. 2008.
- [19] S. Shrestha, J.-J. Park, and D.-Y. Choi, "Rain rate modeling of 1-min from various integration times in South Korea," *SpringerPlus*, vol. 5, no. 1, pp. 1–34, Dec. 2016.
- [20] N. Pérez-García, A. D. Pinto, J. M. Torres, Y. E. Rivera, L. A. D. S. Mello, R. García, E. J. Ramírez, and P. Guevara-Salgado, "Preliminary rain rate statistics with one-minute integration time for radio propagation uses in Venezuela," *Electron. Lett.*, vol. 59, no. 6, Mar. 2023, Art. no. e12725.
- [21] R. Bhattacharya, R. Das, R. Guha and S. D. Barman, "Variability of millimetrewave rain attenuation and rain rate prediction: A survey," *Indian J. Radio Space Phys.*, Vol. 36, pp. 325–344, Aug. 2007.

- [22] A. Paraboni, C. Riva, C. Capsoni, L. Luini, L. Castanet, N. Jeannin, A. Martellucci, M. Pontes, M. Schönhuber, and L. Emiliani, "Propagation modelling and mapping of rain, clouds and water vapour to cope with spatial and temporal variability," in *Proc. 5th Eur. Conf. Antennas Propag. (EUCAP)*, Apr. 2011, pp. 3242–3246.
- [23] *Propagation Data and Prediction Methods Required for the Design of Earth-Space Telecommunication Systems*, document Recommendation ITU-R P.618, International Telecommunication Union, 2023.
- [24] A. M. Al-Saegh, A. Sali, J. S. Mandeep, and A. Ismail, "Extracted atmospheric impairments on earth-sky signal quality in tropical regions at Ku-band," *J. Atmos. Solar-Terrestrial Phys.*, vol. 104, pp. 96–105, Nov. 2013.
- [25] Y. A. Jassim, M. Çevik, and T. A. Elwi, "10 GHz printed circuit antenna for wireless power transfer applications," in *Proc. 5th Int. Congr. Human-Comput. Interact., Optim. Robotic Appl. (HORA)*, Jun. 2023, pp. 1–4.
- [26] M. H. Jwair and T. A. Elwi, "Metasurface antenna circuitry for 5G communication networks," *Infocommun. J., A Publication Sci. Assoc. Infocommun.*, vol. 15, no. 2, pp. 2–7, 2023.
- [27] H. Almizan, M. H. Jwair, Y. Al Naiemy, Z. A. A. Hassain, L. Nagy, and T. A. Elwi, "Novel metasurface based microstrip antenna design for gain enhancement RF harvesting," *Infocommun. J.*, vol. 15, no. 1, pp. 2–8, 2023.
- [28] M. M. Ismail, T. A. Elwi, and A. J. Salim, "Reconfigurable composite right/left-handed transmission line antenna based Hilbert/Minkowski stepped impedance resonator for wireless applications," *Radioelectronic Comput. Syst.*, no. 1, pp. 77–91, Mar. 2023.
- [29] H. H. Al-khaylani, T. A. Elwi, and A. A. Ibrahim, "Optically remote-controlled miniaturized 3D reconfigurable CRLH-printed MIMO antenna array for 5G applications," *Microw. Opt. Technol. Lett.*, vol. 65, pp. 603–610, Feb. 2023.
- [30] A. M. Majeed, T. A. Elwi, and Z. A. A. Hassain, "Defected slots 3D antenna structure for millimeter applications," *Int. J. Ind. Electron. Elect. Eng.*, vol. 10, pp. 6–9, Jan. 2022.
- [31] A. Abdulmjeed, T. A. Elwi, and S. Kurnaz, "Metamaterial Vivaldi printed circuit antenna based solar panel for self-powered wireless systems," *Progress Electromagn. Res.*, vol. 102, pp. 181–192, 2021, doi: 10.2528/PIERM21032406.
- [32] A. Banerjee, K. Vaesen, A. Visweswaran, K. Khalaf, Q. Shi, S. Brebels, D. Guermendi, C.-H. Tsai, J. Nguyen, and A. Medra, "Millimeter-wave transceivers for wireless communication, radar, and sensing," in *Proc. IEEE Custom Integr. Circuits Conf. (CICC)*, vol. 2019, pp. 1–11.
- [33] Y. J. Cheng, H. Xu, D. Ma, J. Wu, L. Wang, and Y. Fan, "Millimeter-wave shaped-beam substrate integrated conformal array antenna," *IEEE Trans. Antennas Propag.*, vol. 61, no. 9, pp. 4558–4566, Sep. 2013.
- [34] V. Semkin, F. Ferrero, A. Bisognin, J. Ala-Laurinaho, C. Luxey, F. Devillers, and A. V. Räsänen, "Beam switching conformal antenna array for mm-wave communications," *IEEE Antennas Wireless Propag. Lett.*, vol. 15, pp. 28–31, 2016.
- [35] V. Semkin, A. Bisognin, M. Kyrö, V.-M. Kolmonen, C. Luxey, F. Ferrero, F. Devillers, and A. V. Räsänen, "Conformal antenna array for millimeter-wave communications: Performance evaluation," *Int. J. Microw. Wireless Technol.*, vol. 9, no. 1, pp. 241–247, Feb. 2017.
- [36] C.-X. Mao, S. Gao, and Y. Wang, "Broadband high-gain beam-scanning antenna array for millimeter-wave applications," *IEEE Trans. Antennas Propag.*, vol. 65, no. 9, pp. 4864–4868, Sep. 2017.
- [37] B. T. P. Madhav, T. Anilkumar, and S. K. Kotamraju, "Transparent and conformal wheel-shaped fractal antenna for vehicular communication applications," *AEU-Int. J. Electron. Commun.*, vol. 91, pp. 1–10, Jul. 2018.
- [38] S. S. S. Kalyan, "Analysis of synthesized Ka-band linear array antenna for beam steering applications," *J. Mech. Continua Math. Sci.*, vol. 13, no. 5, Dec. 2018.
- [39] A. Adhikari, A. Bhattacharya, and A. Maitra, "Rain-induced scintillations and attenuation of Ku-band satellite signals at a tropical location," *IEEE Geosci. Remote Sens. Lett.*, vol. 9, no. 4, pp. 700–704, Jul. 2012.
- [40] A. D. Panagopoulos, P. M. Arapoglou, and P. G. Cottis, "Satellite communications at KU, KA, and V bands: Propagation impairments and mitigation techniques," *IEEE Commun. Surveys Tuts.*, vol. 6, no. 3, pp. 2–14, 3rd Quart., 2004.
- [41] T. V. Omotosho and C. O. Oluwafemi, "Impairment of radio wave signal by rainfall on fixed satellite service on earth-space path at 37 stations in Nigeria," *J. Atmos. Solar-Terr. Phys.*, vol. 71, nos. 8–9, pp. 830–840, Jun. 2009.
- [42] M. Sherif, R. Chowdhury, and A. Shetty, "Rainfall and intensity-duration-frequency (IDF) curves in the United Arab Emirates," in *Proc. World Environ. Water Resour. Congr.*, 2014, pp. 2316–2325.
- [43] A. Chandran, G. Basha, and T. B. M. J. Ouarda, "Influence of climate oscillations on temperature and precipitation over the United Arab Emirates," *Int. J. Climatol.*, vol. 36, no. 1, pp. 225–235, Jan. 2016.
- [44] T. Merabtene, M. Siddique, and A. Shanableh, "Assessment of seasonal and annual rainfall trends and variability in Sharjah City, UAE," *Adv. Meteorol.*, vol. 2016, pp. 1–13, 2016.
- [45] M. Sherif, M. Almulla, A. Shetty, and R. K. Chowdhury, "Analysis of rainfall, PMP and drought in the United Arab Emirates," *Int. J. Climatol.*, vol. 34, no. 4, pp. 1318–1328, Mar. 2014.
- [46] M. Sherif, S. Akram, and A. Shetty, "Rainfall analysis for the northern wadis of United Arab Emirates: A case study," *J. Hydrologic Eng.*, vol. 14, no. 6, pp. 535–544, Jun. 2009.
- [47] M. Almazroui, "Rainfall trends and extremes in Saudi Arabia in recent decades," *Atmosphere*, vol. 11, no. 9, p. 964, Sep. 2020.
- [48] T. V. Omotosho, O. O. Ometan, S. A. Akinwumi, O. M. Adewusi, A. O. Boyo, and M. S. J. Singh, "Year to year variation of rainfall rate and rainfall regime in Ota, Southwest Nigeria for the year 2012 to 2015," *J. Phys., Conf.*, vol. 852, May 2017, Art. no. 012013.
- [49] V. Ramachandran and V. Kumar, "Modified rain attenuation model for tropical regions for Ku-band signals," *Int. J. Satell. Commun. Netw.*, vol. 25, no. 1, pp. 53–67, Jan. 2007.
- [50] P. M. Kalaivaanan, A. Sali, R. S. A. R. Abdullah, S. Yaakob, M. J. Singh, and A. M. Al-Saegh, "Measuring contention and congestion on ad-hoc multicast network towards satellite on Ka-band and LiFi communication under tropical environment region," *IEEE Access*, vol. 8, pp. 108942–108951, 2020.
- [51] J. S. Mandeep, Y. Y. Ng, H. Abdullah, and M. Abdullah, "The study of rain specific attenuation for the prediction of satellite propagation in Malaysia," *J. Infr., Millim., Terahertz Waves*, vol. 31, pp. 681–689, Mar. 2010.
- [52] A. M. Al-Saegh, T. A. Elwi, O. A. Abdullah, A. Sali, and A. H. J. Aljumaily, "Rainfall effect on satellite communications in Mosul at frequencies above 10 GHz," in *Proc. 7th Int. Conf. Space Sci. Commun. (IconSpace)*, Nov. 2021, pp. 318–322.
- [53] *Specific Attenuation Model for Rain for Use in Prediction Methods*, document Recommendation ITU-R P.838, International Telecommunication Union, 2005.
- [54] *Rain Height Model for Prediction Methods*, document Recommendation ITU-R P.839, International Telecommunication Union, 2013.
- [55] J. S. Ojo, S. E. Falodun, and O. Odiba, "0 °C isotherm height distribution for earth-space communication satellite links in Nigeria," *Indian J. Radio Space Phys.*, vol. 43, pp. 225–234, May 2017.
- [56] J. R. Barry, E. A. Lee, and D. G. Messerschmitt, *Digital Communication*. Berlin, Germany: Springer, 2012.
- [57] D. Bala, G. Waliullah, N. Islam, I. Abdullah, and M. A. Hossain, "Analysis the probability of bit error performance on different digital modulation techniques over AWGN channel using MATLAB," *J. Electr. Eng., Electron., Control Comput. Sci.*, vol. 7, pp. 9–18, 2021.
- [58] W. Van Sark, "Design and components of photovoltaic systems," in *Comprehensive Renewable Energy*. Amsterdam, The Netherlands: Elsevier, 2012, pp. 679–695.
- [59] L. J. Ippolito, *Satellite Communications Systems Engineering: Atmospheric Effects, Satellite Link Design and System Performance*. Hoboken, NJ, USA: Wiley, 2017.



**ALI M. AL-SAEGH** received the B.Sc. degree in electronic and communications and the M.Sc. degree in satellite engineering from the Electronic and Communications Engineering Department, Nahrain University, Baghdad, Iraq, in 2005 and 2008, respectively, and the Ph.D. degree in wireless communications engineering from the Computer and Communication System Engineering Department, Universiti Putra Malaysia (UPM), Selangor, Malaysia, in 2015. He is currently an

Associate Professor with the Department of Space Technology Engineering, Middle Technical University, Baghdad. His areas of specialization are satellite communications, atmospheric impairments prediction, channel modeling, LMS communications, antenna and propagation, and fade mitigation techniques.



**FATMA TAHER** (Senior Member, IEEE) received the Ph.D. degree from the Khalifa University of Science, Technology and Research, United Arab Emirates, in 2014. She is currently the Assistant Dean of the College of Technological Innovation, Zayed University, Dubai, United Arab Emirates. She has published more than 40 papers in international journals and conferences. Her research interests include signal and image processing, pattern recognition, deep learning, machine learning,

artificial intelligence, and medical image analysis, especially in detecting of the cancerous cells, kidney transplant, and autism. In addition to that, her researches are watermarking, remote sensing, and satellite images. She served as a member for the steering, organizing, and technical program committees for many international conferences. Her current publication and research interests include image classification, medical image processing, deep learning (artificial intelligence), diseases, image segmentation, neural nets, CAD, internet, the Internet of Things, Markov processes, antenna radiation patterns, artificial intelligence, biomedical MRI, broadband antennas, cancer, cardiology, computer crime, computer network security, computerized tomography, convolutional neural nets, data compression, data structures, diagnostic radiography, discrete cosine transforms, and distributed processing.



**TAHA A. ELWI** was born in 1982. He received the B.Sc. degree from the Electrical Engineering Department, Al-Nahrain University, Baghdad, Iraq, in 2003, the M.Sc. (master's) degree from the Laser and Optoelectronics Engineering Department, Al-Nahrain University, in 2005, and the Ph.D. degree in system engineering and science, in December 2011. From April 2005 to August 2007, he was with Huawei Technologies Company, Baghdad. In January 2008, he joined the

University of Arkansas at Little Rock. He is currently a Research Advisor follow with University Putra Malaysia (UPM), from 2013 to 2014. In 2015, he was a Visiting Professor with New York University, until 2016. He is also the Head of the Communication Department, Al-Mammon University College, from 2016 to 2022. He was considered of Stanford University's top 2% scientists, in 2022 and 2023. His research interests include wearable and implantable antennas for biomedical wireless systems, smart antennas, Wi-Fi deployment, electromagnetic wave scattering by complex objects, design, modeling, testing of metamaterial structures for microwave applications, design and analysis of microstrip antennas for mobile radio systems, precipitation effects on terrestrial and satellite frequency re-use communication systems, effects of the complex media on electromagnetic propagation and GPS, nano-scale structures in the entire electromagnetic spectrum, pattern recognition, signal and image processing, machine learning, deep learning, game theory, and medical image analysis-based artificial intelligence algorithms and classifications. His research is conducted to consider wireless sensor networks based on microwave terminals and laser optoelectronic devices. Also, his work is extended to realize advancements in reconfigurable intelligent surfaces and control the channel performance. Nevertheless, the evaluation of modern physics phenomena in wireless communication networks, including cognitive radio networks and squint effects is currently part of his research. He serves as an Editor for many international journals and publishers, such as MDPI, IEEE, Springer, and Elsevier. Since 2020, he has been the Head of the International Applied and Theoretical Research Center (IATRC), Baghdad Quarter, Iraq. Also, he has been a member of the Iraqi Scientific Research Consultant, since 2016. He is leading three collaborations around the world regarding biomedical applications using artificial intelligence-based microwave technology. He is a supervisor of many funded projects and Ph.D. theses with corresponding of more than 150 published articles and holding ten patents. Seeking a challenging position in the academic developments that leverages my extensive professional and educational experiences to be applied in strategically thinking for building an effective institutional partnership around the world. Areas of focus could include constructing new engineering departments with advanced laboratories. He received the Highest Graduation Award for the B.Sc. and M.Sc. degrees.



**MOHAMMAD ALIBAKHSHIKENARI** (Member, IEEE) received the Ph.D. (European label) degree in electronics engineering from the University of Rome "Tor Vergata," Italy, in February 2020. From May 2018 to December 2018, he was a Ph.D. Visiting Researcher with the Chalmers University of Technology, Gothenburg, Sweden. His training during this Ph.D. research visit included a research stage in the Swedish Company Gap Waves AB, Gothenburg. Since July 2021, he has

been with the Department of Signal Theory and Communications, Universidad Carlos III de Madrid (uc3m), Spain, as a Principal Investigator of the CONEX (CONnecting EXcellence)-Plus Talent Training Program and Marie Skłodowska-Curie Actions. He was also a Lecturer of the Electromagnetic Fields and Electromagnetic Laboratory, Department of Signal Theory and Communications (2021–2022). He received the "Teaching Excellent Acknowledgement" Certificate for the course of electromagnetic fields from the Vice-Rector of Studies with uc3m. From December 2022 to May 2023, he spent three industrial and academic research visits in SARAS Technology Company Ltd., Leeds, England; Edinburgh Napier University, Edinburgh, Scotland; and University of Bradford, West Yorkshire, England, which were defined by CONEX-Plus Talent Training Program and Marie Skłodowska-Curie Actions as his secondment research visit plans. His research interests include electromagnetic systems, antennas and wave-propagations, metamaterials and metasurfaces, sensors, synthetic aperture radars (SAR), 5G and beyond wireless communications, multiple input multiple output (MIMO) systems, RFID tag antennas, substrate integrated waveguides (SIWs), impedance matching circuits, microwave components, millimeter-waves and terahertz integrated circuits, gap waveguide technology, beamforming matrix, and reconfigurable intelligent surfaces (RIS), which led to achieve more than 5400 citations and H-index above 45 reported by Scopus, Google Scholar, and ResearchGate. He was a recipient of the three years Principal Investigator research grant funded by Universidad Carlos III de Madrid and the European Union's Horizon 2020 Research and Innovation Program under the Marie Skłodowska-Curie Grant started, in July 2021, two years postdoctoral research grant funded by the University of Rome "Tor Vergata" started, in November 2019, three years Ph.D. Scholarship funded by the University of Rome "Tor Vergata" started, in November 2016, and two Young Engineer Awards of the 47th and 48th European Microwave Conference were held in Nuremberg, Germany, in 2017, and in Madrid, Spain, in 2018, respectively. In April 2020, his research article titled "High-Gain Metasurface in Polyimide On-Chip Antenna Based on CRLH-TL for Sub Terahertz Integrated Circuits" published in *Scientific Reports* was awarded as the Best Month Paper with the University of Bradford, West Yorkshire, England. He is serving as an Associate Editor for *Radio Science* and *IET Journal of Engineering*. He also acts as a referee in several highly reputed journals and international conferences.



**BAL S. VIRDEE** (Senior Member, IEEE) received the B.Sc. and M.Phil. degrees in communications engineering from the University of Leeds, U.K., and the Ph.D. degree in electronic engineering from the University of London, U.K. He has worked in industry for various companies including Philips, U.K., as a Research and Development Engineer and Teledyne Defence and Space as a Future Products Developer in RF/microwave communications. He has taught at several academic

institutions before joining London Metropolitan University, where he is currently a Senior Professor in communications technology with the School of Computing and Digital Media, where he is also the Head the Communications Technology Research Center. His research, in collaboration with industry and academia, is in wireless communications encompassing mobile-phones to satellite-technology. He has chaired technical sessions at IEEE international conferences and published numerous research papers. He is an Executive Member of IET's Technical and Professional Network Committee on RF/Microwave-Technology. He is a fellow of IET.

**OSAMA ABDULLAH**, photograph and biography not available at the time of publication.

**SALAHUDDIN KHAN**, photograph and biography not available at the time of publication.



**PATRIZIA LIVRERI** (Senior Member, IEEE) received the Laurea degree (Hons.) in electronics engineering and the Ph.D. degree in electronics and communications engineering from the University of Palermo, Italy, in 1986 and 1992, respectively. He is currently a Professor with the Department of Engineering, University of Palermo, and a Visiting Professor with San Diego State University. From 1993 to 1994, she was a Researcher with CNR. Since 1995, she has been the Scientific Director of the Microwave Instruments and Measurements Laboratory, Engineering Department, University of Palermo. In 2020, she also joined the CNIT National Laboratory for Radar and Surveillance Systems RaSS, Pisa. Her research interests include microwave and millimeter vacuum high power (TWT, Klystron) and solid-state power amplifiers for radar applications, high power microwave source (virtual cathode oscillator and magnetically insulated transmission line oscillator), microwave and optical antennas, radar, and microwave quantum radar. She is a Principal Investigator of the “Microwave Quantum Radar” Project, funded by the Ministry of Defense, in 2021. She is a supervisor of many funded project and the author of more than 200 published articles.



**ABDULMAJEED AL-JUMAILY** (Senior Member, IEEE) received the B.Sc. degree (Hons.) in electronics and communication engineering, in 2003, and the M.Sc. degree in wireless communications engineering and the Ph.D. degree in wireless communication and networks engineering from University Putra Malaysia (UPM), in 2014 and 2022, respectively. During the Ph.D. and master's degrees, he was a Research Assistant with the WiPNET Research Centre, Department of Computer and Communication Systems Engineering, Faculty of Engineering, UPM, from the master's days, in 2011, until the completion of the Ph.D. degree, in 2023. His research interests include wireless communications, including mobile communications systems, satellite communications, radio propagation, link budget, WiFi, bluetooth, signal processing, image processing, augmented reality, digital communication, AI, and machine learning. He has research experience conducting experimental applications and measurements in the mobile communications laboratory, which keeps him up to date with the latest developments in the field. He is also responsible for supervising research projects, including the Ph.D., master's theses, and undergraduate projects, and developing successful educational programs and courses that inspire and challenge students. Additionally, he regularly publishes research articles in peer-reviewed journals to share his findings with the scientific community. He is currently a Ph.D. Research Fellow on an Erasmus + KA107 exchange as a Ph.D. Researcher with the University Charles III of Madrid, Spain, from 2022 to 2023. Since 2017, he has been a member of the International Association of Engineers (IAENG). He is also a member of Malaysia's Board of Technologists (MBOT) and the U.K.'s BCS, the Chartered Institute for IT.



**MOHAMED FATHY ABO SREE** received the Master of Science (M.Sc.) from Arab Academy for Science, Technology, and Maritime Transport (AASTMT), Cairo, Egypt, in 2013, and the Ph.D. degree in electrical engineering from Ain Shams University, Egypt, in 2019, thereby solidifying and expanding his expertise. He currently holds the position of an Associate Professor with the Department of Electronics and Communication Engineering, AASTMT, a role he has been fulfilled since 2019. Within this role, he is dedicated to advancing academic excellence in his field. Throughout his academic and professional journey, he has consistently pursued and achieved significant milestones. Actively engaging with the academic community, he participates in the peer-review process for prestigious journals such as IEEE Access and the PIER online journal. This involvement underscores his unwavering commitment to upholding the quality and integrity of scientific contributions within his specialized field. An eminent aspect of his professional profile lies in his prolific publication record. He has authored and co-authored 76 research articles, all indexed in the Science Citation Index (SCI), with an additional seven articles indexed in SCOPUS. This underscores the international recognition garnered by his work. His academic impact is further underscored by an impressive H-index of 10, signifying that he has authored at least 10 papers, each cited a minimum of 10 times. The substantial citation count of 399 reflects the widespread recognition and influence of his contributions within the scholarly community. Notably, the i10 index, representing publications with at least ten citations, aligns seamlessly with his H-index, highlighting the consistency and depth of his scholarly contributions. His commendable H-index and substantial citation count collectively affirm his significant and enduring impact on the academic field.

**ARKAN MOUSA MAJEED**, photograph and biography not available at the time of publication.



**LIDA KOUHALVANDI** (Senior Member, IEEE) received the B.Sc. degree in electronics engineering from the Azad University of Tabriz, Tabriz, Iran, in 2011, the M.Sc. and Ph.D. (Hons.) degrees in electronics engineering from Istanbul Technical University, Istanbul, Turkey, in 2015 and 2021, respectively, and the Associate Professor degree, in February 2023. She joined the Department of Electrical and Electronics Engineering, Dogus University, as an Assistant Professor, in October 2021. In recognition of her research, she received the Doctoral Fellowship with the Department of Electronics and Telecommunications, Politecnico di Torino, Turin, Italy, from 2019 to 2020. She joined Politecnico di Torino, Turin, as a Research Fellowship, from February 2021 to July 2021 and from May 2022 to May 2023. Her research interests include radio frequency and analog engineer are power amplifier, antenna, analog designs, and implantable medical devices. She also has experience in computer-aided designs and optimization algorithms through machine learning. She received “Best Presentation Award” from EExPolytech-2021: Electrical Engineering and Photonics Conference, in 2021. Additionally, her Ph.D. thesis accepted for the presentation at Ph.D. Forum of the 2021 IEEE/ACM Design Automation Conference (DAC 2021) in San Francisco, USA. From the 30th IEEE Conference on Signal Processing and Communications Applications, she received another “Best Paper Award,” in 2022. She received the 2022 Mojgan Daneshmand Grant from the IEEE Antennas and Propagation Society (AP-S), organized by the IEEE AP-S Young Professionals. Additionally, her Ph.D. thesis was awarded by Istanbul Technical University as the “Outstanding Ph.D. Thesis” and also from Turkish Electronics Industrialists Association (TESID) as the “Best Innovation and Creativity Ph.D. Thesis,” in 2022.



**ZAID A. ABDUL HASSAIN** received the B.Eng. degree in electrical engineering from the University of Mustansiriyah, Baghdad, in 2000, and the master's degree in engineering science, in 2002. He is currently a Professor and the Director of Antenna and Microwave with the Department of Electrical Engineering, University of Mustansiriyah.



**GIOVANNI PAU** (Senior Member, IEEE) received the bachelor's degree in telematics engineering from the University of Catania, Italy, and the master's degree (cum laude) in telematics engineering and the Ph.D. degree from the Kore University of Enna, Italy. He is currently an Associate Professor with the Faculty of Engineering and Architecture, Kore University of Enna. He is the author/coauthor of more than 80 refereed articles published in journals and conference proceedings.

He is a member of the IEEE (Italy Section) and has been involved in several international conferences as the session co-chair and a technical program committee member. He serves/served as a leading guest editor in special issues for several international journals. He is an Editorial Board Member as an Associate Editor of several journals, such as *IEEE Access*, *Wireless Networks* (Springer), *EURASIP Journal on Wireless Communications and Networking* (Springer), *Wireless Communications and Mobile Computing* (Hindawi), *Sensors* (MDPI), and *Future Internet* (MDPI), to name a few. His research interests include wireless sensor networks, fuzzy logic controllers, intelligent transportation systems, the Internet of Things, smart homes, and network security.

...